Macromolecules

ARTICLE

pubs.acs.org/Macromolecules

Crystalline Low-Band Gap Polymers Comprising Thiophene and 2,1,3-Benzooxadiazole Units for Bulk Heterojunction Solar Cells

Jian-Ming Jiang, Po-An Yang, Tsung-Hsuan Hsieh, and Kung-Hwa Wei*

Department of Materials Science and Engineering, National Chiao Tung University, 300 Hsinchu, Taiwan

ABSTRACT: We have used Stille coupling polymerization to synthesize a series of new crystalline low−band gap conjugated polymers—**PTHBO**, **PBTTBO**, and **PTTTBO**—constituting mainly electron-rich thiophene (**TH**), 2,2′-bithiophene (**BT**), and thieno[3,2-*b*]thiophene (**TT**) units in conjugation with electron-deficient 2,1,3-benzooxadiazole (**BO**) moieties. All of these polymers exhibited (i) sufficient energy offsets with respect to those of fullerenes to allow efficient charge transfer and (ii) low-lying highest occupied molecular orbital (HOMO, −5.47 eV). These polymers exhibited excellent thermal stability, high crystallinity, and broad spectral absorptions. As a result, bulk heterojunction photovoltaic devices derived from these polymers and fullerenes provided open-circuit voltages (V_{oc}) as high as 1.02 V. In particular, the photovoltaic device comprising the **PTTTBO**/$PC_{61}BM$ (1:1) blend system and 1,8-diiodooctane (DIO, 0.5 vol %) as an additive exhibited excellent performance, under AM 1.5 G irradiation (100 mW cm^{-2}), with a value of V_{oc} of 0.85 V, a short-circuit current density (J_{sc}) of 11.6 mA cm^{-2}, a fill factor (FF) of 0.54, and a promising power conversion efficiency (PCE) of 5.3%.

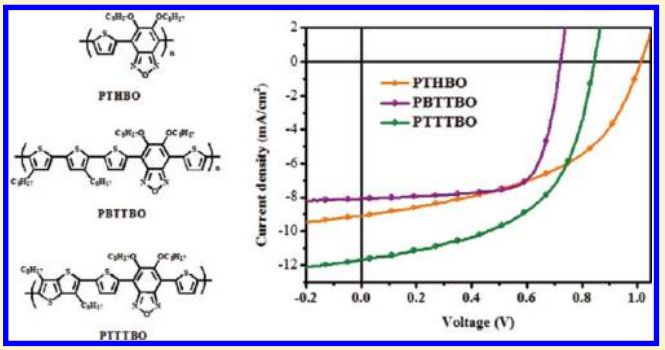

INTRODUCTION

Thin-film polymer solar cells (PSCs) based on bulk heterojunction (BHJ) structures incorporating (i) conjugated polymers possessing delocalized π electrons and (ii) fullerenes are being studied extensively because they allow the fabrication of lightweight, large-area, flexible devices using low-cost solution processing methods.[1−4] Regioregular polythiophene derivatives have been widely investigated for BHJ devices because of their high crystallinity, good light harvesting in the visible spectrum, and excellent carrier mobility.[5−8] Nevertheless, the power conversion efficiencies (PCEs) of such systems are difficult to improve upon because of the limited absorption at wavelengths of less than 650 nm[9] and because the open-circuit voltage (V_{oc}) is limited at approximately 0.6 V.

In attempts to harvest more photons and to tune the energy levels, several conjugated polymers have been developed featuring electron donor/acceptor (D/A) units in the main chain conjugated configurations[10−16] and side chain−attached architectures.[17−20] Recently, some new low−band gap polymers have exhibited PCEs of up to 7%.[21−25] To obtain high-performance photovoltaic polymer materials, it will be necessary to synthesize conjugated polymers with several ideal properties: low band gaps to broaden the absorption range; crystalline characteristics to ensure good charge mobility; low highest occupied molecular orbital (HOMO) energy levels to enhance the values of V_{oc}; and suitable lowest unoccupied molecular orbital (LUMO) energy levels for efficient electron transfer to the fullerene moieties.

Strong electron-withdrawing units are necessary when choosing an acceptor unit to lower the LUMO energy level of a D/A polymer. With a proper selection of the acceptor, however, both the HOMO and LUMO energy level of the synthesized polymer can be decreased. Benzothiadiazole (BT) is one of the stronger electron-withdrawing moieties used widely in PSCs exhibiting PCEs of up to 5−6%,[26] due to a combination of its electron accepting properties and its ability to adopt a quinoid structure, resulting in low−band gap, coplanar polymers. Replacing the sulfur atom with an oxygen atom forms benzooxadiazole (BO), which can decrease both the HOMO and LUMO energy levels;[27] this molecular structure not only can result in air-stable polymers but also produce high open-circuit potentials when blended with fullerenes.[28] Some polymers based on BO units, however, provide low PCEs—presumably the result of their relatively low molecular weights and low solubility,[27,29] while other polymers incorporating BO units had decent molecular weight and exhibited good device PCE using additives.[30] To solve this problem, we designed a soluble acceptor[31] by introducing two octyloxy chains on the BO ring.

In this study, we selected several thiophene-based building blocks so that our D/A polymers would feature not only strong and broad absorption (i.e., good harvesting of sunlight) but also suitable molecular energy levels to ensure good charge separation and transportation as well as high open-circuit voltages. Furthermore, we expected the development of new D/A polymers exhibiting crystalline characteristics to lead to significantly enhanced charge mobilities in the active layers of the devices. Several p-type conjugated polymers containing the symmetrical

Received: August 12, 2011
Revised: October 18, 2011
Published: November 08, 2011

thiophene, bi(alkyl)thiophene[32−34] and 3,6-dialkylthieno[3,2-b]thiophene[35] exhibit crystalline characteristics and high hole mobilities when used in organic field effect transistors. Considering not only electronic energy levels but also hole mobilities, we prepared a series of new D/A polymers—**PTHBO**, **PBTTBO**, and **PTTTBO**—wherein electron-withdrawing BO units were conjugated with the symmetrical electron-donating units to provide crystalline characteristics and a low-lying HOMO energy levels. Because of these desirable features, we expected **PTHBO**, **PBTTBO**, and **PTTTBO** to exhibit good hole mobilities and high values of V_{oc} when used in photovoltaic applications.

EXPERIMENTAL SECTION

Materials and Synthesis. 2,5-Bis(trimethylstannyl)thiophene (**M3**),[36] (4,4′-dioctyl-2,2′-bithiophene-5,5′-diyl)bis(trimethylstannane) (**M4**),[32] and (3,6-dioctylthieno[3,2-*b*]thiophene-2,5-diyl)bis(trimethylstannane) (**M5**)[13] were prepared according to reported procedures. [6,6]-Phenyl-C_{61}-butyric acid methyl ester ($PC_{61}BM$) was purchased from Nano-C. All other reagents were used as received without further purification, unless stated otherwise.

1,2-Bis(octyloxy)benzene ***(1)***. A mixture of catechol (10 g, 0.091 mol), 1-bromooctane (40 g, 36 mL, 0.21 mol), and K_2CO_3 (38 g, 0.27 mol) in dry DMF (50 mL) was stirred at 100 °C under a N_2 atmosphere for 40 h. After cooling to room temperature, water (300 mL) was added; the organic layer was separated and the aqueous layer extracted with CH_2Cl_2. The combined organic phases were dried ($MgSO_4$) and concentrated under reduced pressure. The crude product was purified through column chromatography (SiO_2, hexane) to provide a colorless oil (27 g, 90%). ^{1}H NMR (300 MHz, $CDCl_3$): δ 6.89 (s, 2H), 3.99 (t, J = 6.9 Hz, 4H), 1.84−1.77 (m, 4H), 1.49−1.29 (m, 20H), 0.90 (t, J = 6.7 Hz, 6H). ^{13}C NMR (75 MHz, $CDCl_3$): δ 149.1, 120.9, 114.0, 69.2, 31.8, 29.4, 29.3, 29.2, 26.0, 22.6, 14.0.

1,2-Dinitro-4,5-bis(octyloxy)benzene ***(2)***. A 65% HNO_3 (20 mL) sample was added dropwise to a two-neck round-bottom flask containing 1,2-bis(octyloxy)benzene (10 g, 30 mmol), CH_2Cl_2 (140 mL), and AcOH (140 mL), cooled at 10 °C . The reaction mixture was warmed to room temperature and stirred for 1 h. The mixture was then cooled to 10 °C and 100% HNO_3 (50 mL) was added dropwise. The mixture was warmed to room temperature and stirred for 40 h before being poured into ice−water. The CH_2Cl_2 layer was separated and the aqueous phase extracted with CH_2Cl_2. The organic phases were combined, washed sequentially with water, sat. $NaHCO_3$ (aq), and brine, and then dried ($MgSO_4$). Concentration under vacuum gave a crude product that was recrystallized from EtOH. Yield: 12 g (95%). ^{1}H NMR (300 MHz, $CDCl_3$): δ 7.29 (s, 2H), 4.09 (t, J = 6.6 Hz, 4H), 1.91−1.81 (m, 4H), 1.49−1.28 (m, 20H), 0.89 (t, J = 6.9 Hz, 6H). ^{13}C NMR (75 MHz, $CDCl_3$): δ 151.7, 136.4, 107.8, 74.7, 31.7, 30.1, 29.4, 29.2, 25.7, 22.6, 14.1.

5,6-Bis(octyloxy)benzo[c][1,2,5]oxadiazole ***(3)***. A mixture of 1,2-dinitro-4,5-bis(octyloxy)benzene (**2**, 848 mg, 2.00 mmol), NaN_3 (650 mg, 10.0 mmol), and *n*-Bu_4NBr (130 mg, 0.400 mmol) was heated under reflux in toluene (10 mL) for 12 h. At this point, the starting material had been consumed (TLC); PPh_3 (630 mg, 2.40 mmol) was added and the mixture heated under reflux for an additional 24 h. The reaction mixture was cooled to room temperature and filtered through a short silica plug; the plug was rinsed with CH_2Cl_2. Evaporation of the solvents from the combined organic phases, under reduced pressure, afforded a crude solid that was recrystallized (EtOH) to yield an off-white solid (683 mg, 63%). ^{1}H NMR (300 MHz, $CDCl_3$): δ 6.79 (s, 2H), 4.05 (t, J = 6 Hz, 4H), 1.92−1.83 (m, 4H), 1.54−1.28 (m, 20H), 0.89 (t, J = 6.7 Hz, 6H). ^{13}C NMR (75 MHz, $CDCl_3$): δ 151.1, 146.7, 90.5, 69.3, 31.7, 29.2, 29.1, 28.5, 25.9, 22.6, 14.0.

4,7-Dibromo-5,6-bis(octyloxy)benzo[c][1,2,5]oxadiazole ***(4, M1)***. AcOH (10 mL) and Br_2 (0.850 mL, 16.6 mmol) were added sequentially to a solution of 5,6-bis(octyloxy)benzo[*c*][1,2,5]oxadiazole (**3**, 1.50 g, 4.00 mmol) in CH_2Cl_2 (80 mL). The resulting mixture was stirred in the dark for 3 days at room temperature and then poured into aqueous NaOH solution (10 g in 200 mL). The aqueous phase was extracted with CH_2Cl_2; the combined organic extracts were washed with brine and concentrated under reduced pressure to afford a crude solid that was purified through column chromatography [SiO_2, hexane/CH_2Cl_2, 9:1 (v/v)] to yield a white solid (2.2 g, 79%). ^{1}H NMR (300 MHz, $CDCl_3$): δ 4.13 (t, J = 9 Hz, 4H), 1.89−1.80 (m, 4H), 1.53−1.29 (m, 20H), 0.88 (t, J = 6.6 Hz, 6H). ^{13}C NMR (75 MHz, $CDCl_3$): δ 155.6, 147.4, 99.5, 75.3, 31.7, 30.1, 29.3, 29.2, 25.8, 22.6, 14.0.

5,6-Bis(octyloxy)-4,7-di(thien-2-yl)benzo[c][1,2,5]oxadiazole ***(5)***. 2-Tributylstannylthiophene (994 μL, 3.13 mmol) was added to a solution of 4,7-dibromo-5,6-bis(octyloxy)benzo[*c*][1,2,5]oxadiazole (4, 665 mg, 1.25 mmol), tris(dibenzylideneacetone)dipalladium ($Pd_2(dba)_3$; 46 mg, 0.050 mmol), and tri-*o*-tolylphosphine (122 mg, 0.400 mmol) in dry toluene (10 mL) and then the reaction mixture was heated under reflux for 16 h under N_2. The reaction mixture was concentrated directly under vacuum. Dry column chromatography [SiO2, hexane/CHCl3, 10:1 (v/v)] afforded a yellow solid (470 mg, 70%). ^{1}H NMR (300 MHz, $CDCl_3$): δ 8.46 (d, J = 3.6 Hz, 2H), 7.50 (d, J = 6.3 Hz, 2H), 7.22 (t, J = 4.5 Hz, 2H), 4.14 (t, J = 7.2 Hz, 4H), 2.05−1.95 (m, 4H), 1.47−1.30 (m, 20H), 0.90 (t, J = 3.3 Hz, 6H). ^{13}C NMR (75 MHz, $CDCl_3$): δ 151.6, 146.7, 132.8, 130.8, 128.0, 127.1, 113.0, 74.4, 31.8, 30.2, 29.5, 29.2, 25.8, 22.6, 14.0.

4,7-Bis(5-bromothien-2-yl)-5,6-bis(octyloxy)benzo[c][1,2,5]oxadiazole ***(M2)***. NBS (355 mg, 2.00 mmol) was added in one portion to a solution of 5,6-bis(octyloxy)-4,7-di(thien-2-yl)benzo[*c*][1,2,5]oxadiazole (**5**, 540 mg, 1.00 mmol) in $CHCl_3$ (40 mL), and glacial AcOH (40 mL) and then the mixture was stirred at room temperature for 20 h in the dark. The solution was concentrated directly onto Celite under vacuum. Dry column chromatography [SiO_2, hexane/$CHCl_3$, 9:1 (v/v)] afforded an orange solid (800 mg, 92%). ^{1}H NMR (300 MHz, $CDCl_3$): δ 8.22 (d, J = 4.2 Hz, 2H), 7.15 (d, J = 4.5 Hz, 2H), 4.14 (t, J = 7.5 Hz, 4H), 2.04−1.94 (m, 4H), 1.47−1.30 (m, 20H), 0.90 (t, J = 2.4 Hz, 6H). ^{13}C NMR (75 MHz, $CDCl_3$): δ 151.1, 146.1, 134.2, 131.1, 130.0, 116.3, 112.6, 74.7, 31.7, 30.1, 29.4, 29.2, 25.7, 22.6, 14.1. Anal. Calcd: C, 51.58; H, 5.48; N, 4.01. Found: C, 51.44; H, 5.47; N, 4.15.

General Procedure for Stille Polymerization. *Alternating Polymer* ***PTHBO***. **M1** (100 mg, 0.187 mmol), **M3** (76.6 mg, 0.187 mmol), and tri(*o*-tolyl)phosphine (4.5 mg, 8.0 mol %) were dissolved in dry toluene (4 mL) and degassed for 15 min. $Pd_2(dba)_3$ (3.4 mg, 2.0 mol %) was added under N_2 and then the reaction mixture was heated at 110 °C for 48 h. After cooling to room temperature, the solution was added dropwise into MeOH (100 mL). The crude polymer was collected, dissolved in $CHCl_3$, and reprecipitated in MeOH. The solid was washed with MeOH, acetone, and $CHCl_3$ in a Soxhlet apparatus. The $CHCl_3$ solution was concentrated and then added dropwise into MeOH. Finally, the polymer was collected and dried under vacuum to give **PTHBO** (70 mg, 80%). ^{1}H NMR (300 MHz, $CDCl_3$): δ 8.68−8.57 (m, 2H), 4.41−4.27 (m, 4H), 2.63−1.21 (m, 24H), 0.97 (s, 6H). Anal. Calcd: C, 68.09; H, 8.35; N, 6.11. Found: C, 67.25; H, 8.18; N, 6.03.

Alternating Polymer ***PBTTBO***. Using a polymerization procedure similar to that described above for **PTHBO**, a mixture of **M2** (100 mg, 0.143 mmol) and **M4** (102 mg, 0.143 mmol) in dry toluene (4 mL) was polymerized to give **PBTTBO** (93 mg, 70%). ^{1}H NMR (300 MHz, $CDCl_3$): δ 8.57−8.02 (m, 4H), 7.07−6.57 (m, 2H), 3.96 (br, 4H), 2.45 (br, 4H), 1.56−0.96 (m, 48H), 0.89 (s, 12H). Anal. Calcd: C, 69.78; H, 8.24; N, 3.01. Found: C, 69.65; H, 8.17; N, 2.87.

Alternating Polymer ***PTTTBO***. Using a polymerization procedure similar to that described above for **PTHBO**, a mixture of **M2** (100 mg,

Scheme 1. Synthesis and Structures of the Monomers

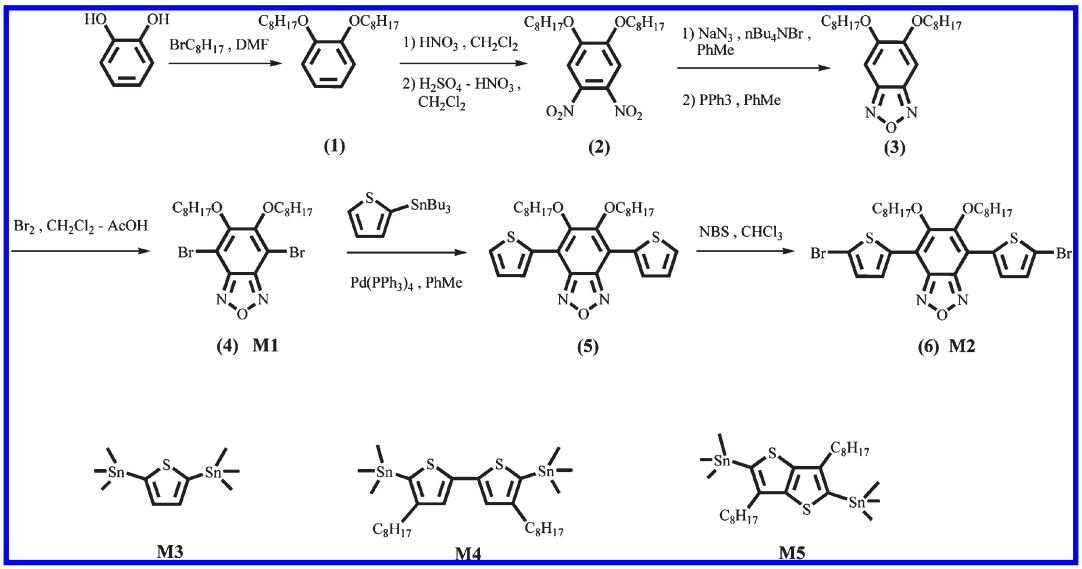

0.143 mmol) and **M5** (98.8 mg, 0.143 mmol) in dry toluene (4 mL) was polymerized to give **PTTTBO** (84 mg, 65%). ^{1}H NMR (300 MHz, $CDCl_3$): δ 8.53−8.12 (m, 4H), 4.01 (br, 4H), 2.57 (br, 4H), 2.72−1.17 (m, 48H), 0.85 (s, 12H). Anal. Calcd: C, 69.13; H, 8.26; N, 3.10. Found: C, 67.85; H, 8.08; N, 2.95.

Measurements and Characterization. ^{1}H NMR spectra were recorded using a Varian UNITY 300-MHz spectrometer. Thermogravimetric analysis (TGA) was performed using a TA Instruments Q500; the thermal stabilities of the samples were determined under a N_2 atmosphere by measuring their weight losses while heating at a rate of 20 °C min^{-1}. Size exclusion chromatography (SEC) was performed using a Waters chromatography unit interfaced with a Waters 1515 differential refractometer; polystyrene was the standard; the temperature of the system was set at 45 °C and THF was the eluent. UV−Vis spectra of dilute samples in dichlorobenzene (DCB) solutions (1×10^{-5} M) were recorded at ca. 25 and 60 °C using a Hitachi U-4100 spectrophotometer. Solid films for UV−Vis spectroscopic analysis were obtained by spin-coating the polymer solutions onto a quartz substrate. Cyclic voltammetry (CV) of the polymer films was performed using a BAS 100 electrochemical analyzer operated at a scan rate of 50 mV s^{-1}; the solvent was anhydrous MeCN, containing 0.1 M tetrabutylammonium hexafluorophosphate ((TBA)PF_6) as the supporting electrolyte. The potentials were measured against a Ag/Ag^+ (0.01 M $AgNO_3$) reference electrode; the ferrocene/ferrocenium ion (Fc/Fc^+) pair was used as the internal standard (0.09 V). The onset potentials were determined from the intersection of two tangents drawn at the rising and background currents of the cyclic voltammograms. HOMO and LUMO energy levels were estimated relative to the energy level of the ferrocene reference (4.8 eV below vacuum level). X-ray diffraction patterns of the pristine polymer thin films were measured using a Bruker D8 high-resolution X-ray diffractometer operated in grazing incidence mode. Topographic and phase images of the polymer:$PC_{61}BM$ films (surface area: 5×5 μm^2) were obtained using a Digital Nanoscope III atomic force microscope operated in the tapping mode under ambient conditions. The thickness of the active layer of the device was measured using a Veeco Dektak 150 surface profiler.

Fabrication and Characterization of Photovoltaic Devices. Indium tin oxide (ITO)−coated glass substrates were cleaned stepwise in detergent, water, acetone, and isopropyl alcohol (ultrasonication; 20 min each) and then dried in an oven for 1 h; subsequently, the substrates were treated with UV ozone for 30 min prior to use. A thin layer (ca. 20 nm) of poly(ethylenedioxythiophene):polystyrenesulfonate (PEDOT:PSS, Baytron P VP AI 4083) was spin-coated (5000 rpm) onto the ITO substrates. After baking at 140 °C for 20 min in air, the substrates were transferred to a N_2-filled glovebox. The polymer and $PC_{61}BM$ were codissolved in DCB at various weight ratios, but with a fixed total concentration (40 mg mL^{-1}). The blend solutions were stirred continuously for 12 h at 80 °C and filtered through a PTFE filter (0.2 μm); the photoactive layers were obtained by spin-coating (600−2000 rpm, 60 s) the blend solutions onto the ITO/PEDOT:PSS surfaces and then heating for 20 min at 100 °C. The thicknesses of the photoactive layers were approximately 85−105 nm. The devices were ready for measurement after thermal deposition (pressure: ca. 1×10^{-6} mbar) of a 20 nm-thick film of Ca and then a 100 nm-thick Al film as the cathode. The effective layer area of one cell was 0.04 cm^2. The current density−voltage ($J-V$) characteristics were measured using a Keithley 2400 source meter. The photocurrent was measured under simulated AM 1.5 G illumination at 100 mW cm^{-2} using a Xe lamp−based Newport 66902 150-W solar simulator. A calibrated Si photodiode with a KG-5 filter was employed to confirm the illumination intensity. External quantum efficiencies (EQEs) were measured using an SRF50 system (Optosolar, Germany). A calibrated monosilicon diode exhibiting a response at 300−800 nm was used as a reference. For hole mobility measurements, hole-only devices were fabricated having the structure ITO/PEDOT:PSS/polymer/Au. The hole mobility was determined by fitting the dark $J-V$ curve into the space-charge-limited current (SCLC) method,[17,37] based on the equation

$$J = \frac{9}{8}\varepsilon_0\varepsilon_r\mu_h\frac{V^2}{L^3}$$

where ε_0 is the permittivity of free space, ε_r is the dielectric constant of the material, μ_h is the hole mobility, V is the voltage drop across the device, and L is the thickness of active layer.

RESULTS AND DISCUSSION

Synthesis and Characterization of the Polymers. Schemes 1 and 2 outline our general synthetic strategy for obtaining the monomers and the polymers. To ensure the good solubility of the BO derivative **M1**, we positioned two octyloxy chains on the BO ring. We synthesized **M3**, **M4**, and **M5** using reported methods.[13,32,36] After Stille couplings using $Pd_2(dba)_3$

Scheme 2. Synthesis and Structures of the Polymers PTHBO, PBTTBO, and PTTTBO

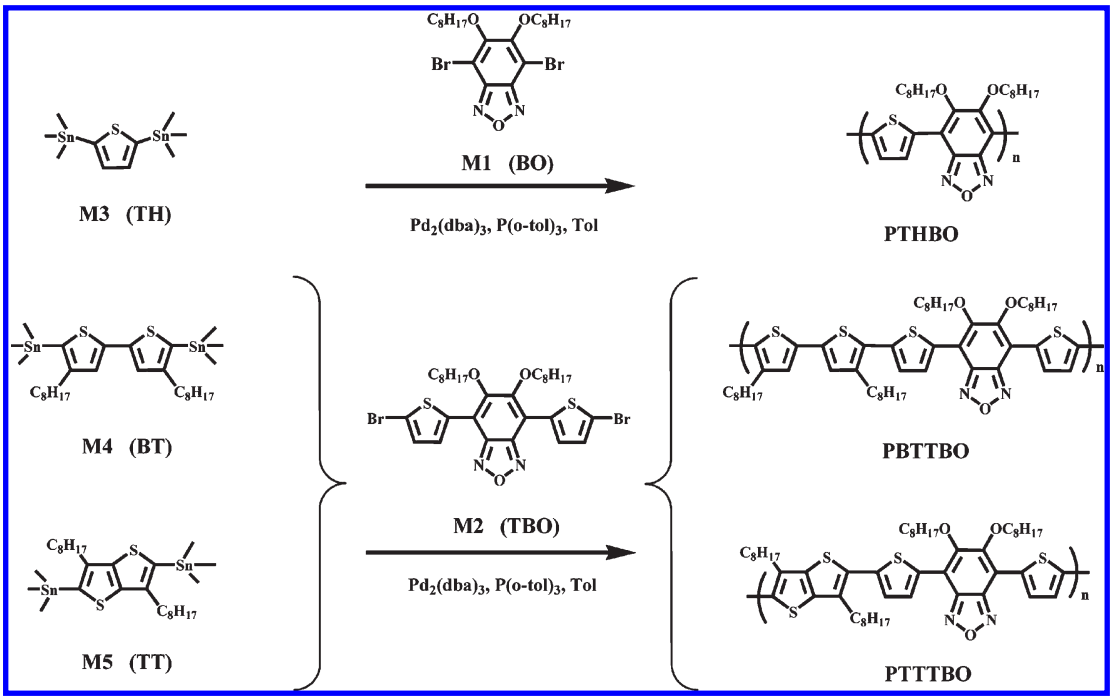

Table 1. Molecular Weights, Thermal Properties, and Hole Mobility of the Polymers

polymer	M_w[a] (KDa)	M_n[a] (KDa)	PDI[a]	T_d[b] (°C)	mobility[c] ($cm^2\ V^{-1}\ s^{-1}$)
PTHBO	52.8	35.2	1.5	310	9.7×10^{-4}
PBTTBO	72.4	42.6	1.7	312	2.2×10^{-3}
PTTTBO	74.7	41.5	1.8	315	1.2×10^{-3}

[a] Values of M_n, M_w, and PDI of the polymers were determined through GPC (polystyrene standards; THF). [b] The 5% weight-loss temperatures in air. [c] The measurement of hole mobility by the SCLC method.

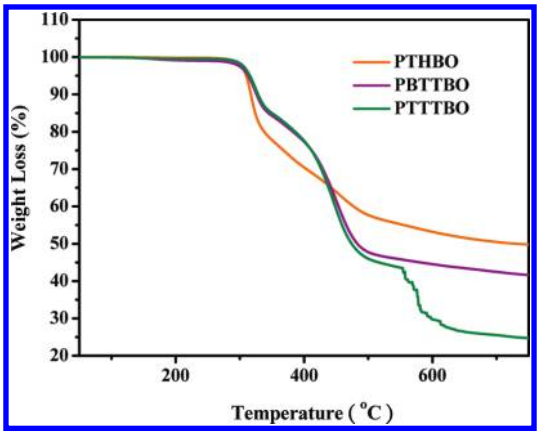

Figure 1. TGA thermograms of the polymers **PTHBO**, **PBTTBO**, and **PTTTBO**, recorded at a heating rate of 20 °C min^{-1} under a N_2 atmosphere.

as catalyst in toluene at 110 °C for 48 h, we obtained the polymers **PTHBO**, **PBTTBO**, and **PTTTBO** in yields of 65−80%. The highest concentration of the copolymers in tetrahydrofuran (THF), chloroform, chlorobenzene, and DCB at room temperature is 25 mg mL^{-1}. We determined the weight-average molecular weights (M_w) of these polymers (Table 1) through Size exclusion chromatography (SEC), against polystyrene standards, in THF as the eluent.

Thermal Stability. We used TGA to determine the thermal stability of the polymers (Figure 1). In air, the 5% weight-loss temperatures (T_d) of **PTHBO**, **PBTTBO**, and **PTTTBO** were 310, 312, and 315 °C, respectively. Thus, they all exhibited good thermal stability against O_2—an important characteristic for device fabrication and application.

Optical Properties. We recorded the normalized optical UV−Vis absorption spectra of the polymers from their dilute DCB solutions at room temperature, hot DCB (60 °C) and as spin-coated films on quartz substrates. Parts a and b of Figure 2 display the absorption spectra of **PTHBO**, **PBTTBO**, and **PTTTBO** in DCB at room temperature and at hot DCB; Table 2 summarizes the optical data, including the absorption peak wavelengths ($\lambda_{max,abs}$), absorption edge wavelengths ($\lambda_{edge,abs}$), and the optical band gap (E_g^{opt}). All of the absorption spectra recorded from dilute DCB solutions feature two absorption bands: one at 300−450 nm, which we assign to localized $\pi-\pi^*$ transitions, and another broader band from 450 to 700 nm in the long wavelength region, corresponding to intramolecular charge transfer (ICT) between the acceptor (BO) and donor (thiophene derivatives) units. And while the absorption spectra blue shift by about 10, 16, and 38 nm for **PTHBO**, **PBTTBO**, and **PTTTBO** in hot DCB (60 °C), respectively, as compared to that in DCB at room temperature, the interchain association band for **PTHBO** still remains at a higher relative intensity than that for **PBTTBO** and **PTTTBO**. This absorption behavior indicated that **PTHBO** aggregates in solution more strongly than **PBTTBO** and **PTTTBO**. The absorption spectra of **PBTTBO** and **PTTTBO** in hot DCB showed exactly the same peak was due to the similar molecular structure of 2,2′-bithiophene (BT) to thieno[3,2-*b*]thiophene (TT). The absorption spectra

dx.doi.org/10.1021/ma201848z |*Macromolecules* 2011, 44, 9155–9163

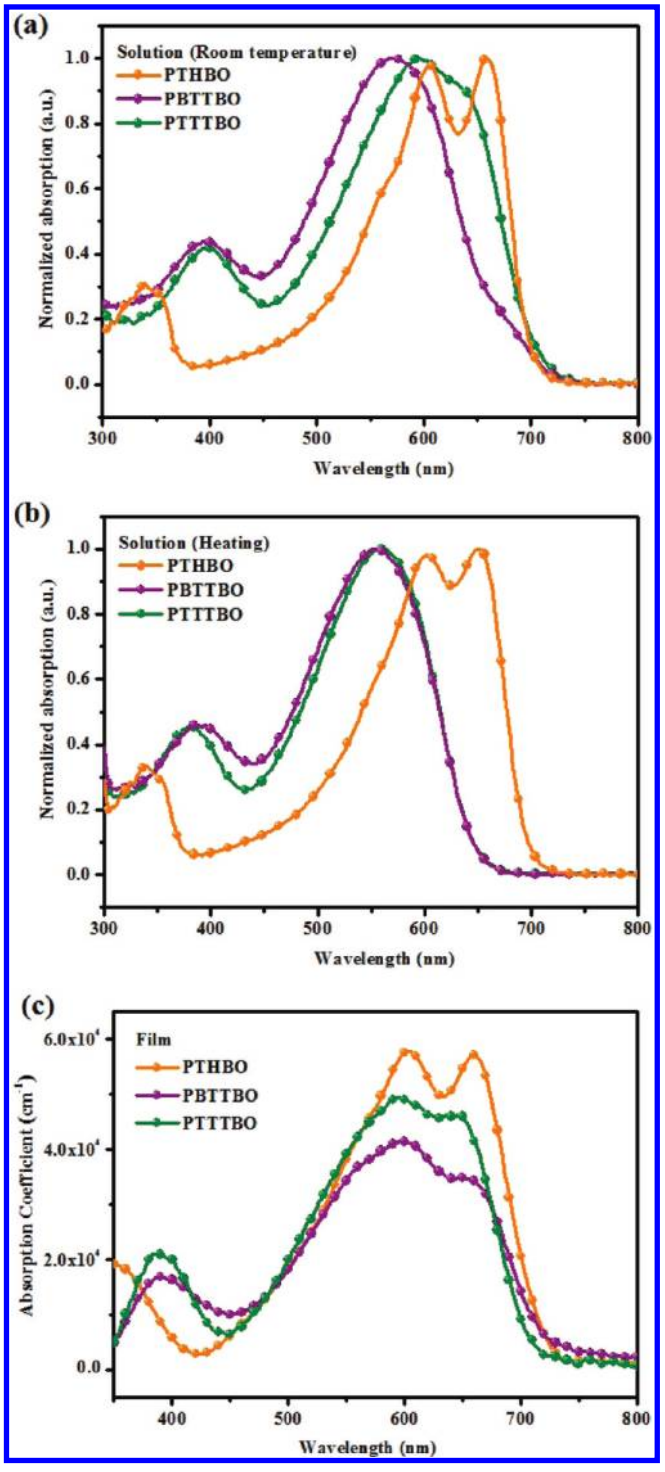

Figure 2. UV−vis absorption spectra of the polymers **PTHBO**, **PBTTBO**, and **PTTTBO** (a) in dilute DCB solutions (1×10^{-5} M) at room temperature, (b) in hot DCB (60 °C), and (c) as solid films.

of the three polymers in the solid state were similar to their corresponding solution spectra, with slight red-shifts (ca. 3−40 nm) of their absorption maxima, indicating that some intermolecular interactions existed in the solid state. In addition, **PBTTBO** and **PTTTBO** displayed a vibronic shoulders at 657 and 648 nm, respectively, implying an ordered arrangement in their solid films, with strong $\pi-\pi$ stacking between the polymeric backbones—a

Table 2. Optical properties of PTHBO, PBTTBO, and PTTTBO

	$\lambda_{max,abs}$ (nm)			λ_{onset} (nm)	
	solution				
	room temp	heating	film	film	E_g^{opt} (eV)
PTHBO	605, 660	602, 650	605, 662	724	1.71
PBTTBO	574	558	600	726	1.70
PTTTBO	596	558	600	720	1.72

feature that also appears in the spectra of regioregular poly(3-hexylthiophene) (P3HT). The absorption edges for **PTHBO**, **PBTTBO**, and **PTTTBO** (Table 2) correspond to optical band gaps (E_g^{opt}) of 1.71, 1.7, and 1.72 eV, respectively.

Electrochemical Properties. The electrochemical properties of the thiophene derivative- benzooxadiazole based copolymers were examined by cyclic voltammetry (CV). Using this technique the energy levels of the copolymer such as HOMO and LUMO can be determined. Figure 3 displays the electrochemical properties of the polymers as solid films; Table 3 summarizes the relevant data. Partially reversible n-doping/dedoping (reduction/reoxidation) processes occurred for these polymers in the negative potential range—except for **PBTTBO**, which underwent an irreversible reduction. In addition, reversible p-doping/dedoping (oxidation/rereduction) processes occurred in the positive potential range for each of these polymers. The onset oxidation potentials (E_{onset}^{ox}, vs Ag/Ag^+) for **PTHBO**, **PBTTBO**, and **PTTTBO** were 0.67, 0.33, and 0.48 V, respectively. The highest onset oxidation potential for **PTHBO** indicates that neighboring electron-deficient units do lead to better accepting properties, but the effect is small because of steric hindrance and the diluting segments between the electron donating/withdrawing moieties. In the reductive potential region, the onset reduction potentials (E_{onset}^{red}) for **PTHBO**, **PBTTBO**, and **PTTTBO** were −1.21, −1.8, and −1.74 V, respectively. On the basis of these onset potentials, we estimated the HOMO and LUMO energy levels according to the energy level of the ferrocene reference (4.8 eV below vacuum level).[38−40] The HOMO energy levels of **PTHBO**, **PBTTBO**, and **PTTTBO** were −5.47, −5.13, and −5.28 eV, respectively, implying that they varied with respect to the modulated ICT strengths resulting from the presence of electron donors with various electron-donating abilities.[41−43] The LUMO energy levels of **PTHBO**, **PBTTBO**, and **PTTTBO** were all located within a reasonable range (from −3.0 to −3.59 eV, Figure 4) and were significantly greater than that of $PC_{61}BM$ (ca. 4.1 eV); thus, we would expect efficient charge transfer/dissociation to occur in their corresponding devices.[44−46] In addition, the electrochemical band gaps (E_g^{ec}) of **PTHBO**, **PBTTBO**, and **PTTTBO**, estimated from the difference between the onset potentials for oxidation and reduction, were in the range 1.88−2.22 eV; i.e., they were slightly larger than the corresponding optical band gaps. This discrepancy between the electrochemical and optical band gaps presumably resulted from the exciton binding energies of the polymers and/or the interface barriers for charge injection.[47]

X-ray Diffraction Patterns. We confirmed the crystalline characteristic of thin films of these polymers from their grazing-incidence X-ray diffraction patterns (Figure 5). The (100), (200), and (300) diffraction peaks for **PBTTBO** appeared at 4.5°, 9°, and 13.5°, respectively, indicating a highly ordered structure with a *d*-spacing of 19.8 Å, ascribable to the interchain

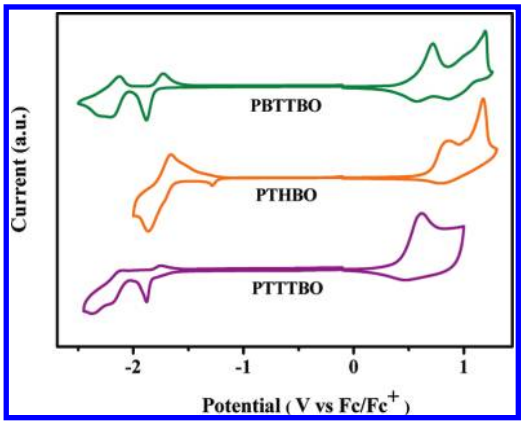

Figure 3. Cyclic voltammograms of the polymers **PTHBO**, **PBTTBO**, and **PTTTBO** as solid films.

Table 3. Electrochemical Properties of PTHBO, PBTTBO, and PTTTBO

	E_{onset}^{ox} (V)	E_{onset}^{red} (V)	HOMO (eV)	LUMO (eV)	E_g^{ec} (eV)
PTHBO	0.67	−1.21	−5.47	−3.59	1.88
PBTTBO	0.33	−1.80	−5.13	−3.00	2.13
PTTTBO	0.48	−1.74	−5.28	−3.06	2.22

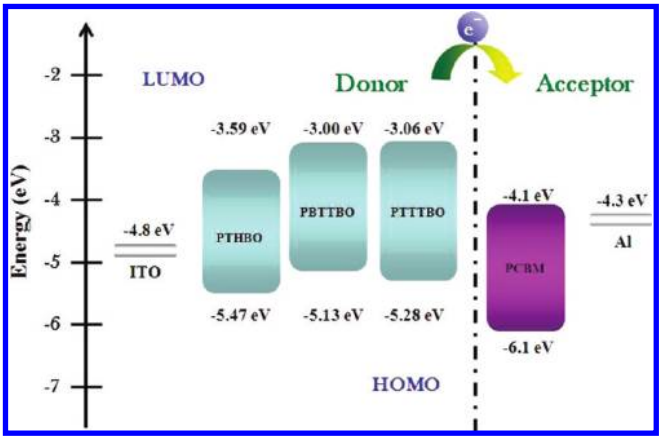

Figure 4. Energy level diagrams for **PTHBO**, **PBTTBO**, and **PTTTBO**.

separation of the alkyl side chains; we assign a broad feature at 24.4°, corresponding to a short distance of 3.6 Å, to facial $\pi-\pi$ stacking of the polymeric backbones. The diffraction pattern of **PTTTBO** featured a sharp diffraction peak at 4.5°, which we assign to its (100) crystal plane (the *d*-spacing of 19.8 Å corresponds to the interchain separation defined by its alkyl side chains); we assign the broad reflection at 23° to its (010) crystal plane, corresponding to a distance of 3.8 Å, suggesting facial $\pi-\pi$ stacking of the polymeric chains. In **PTHBO**, it only shows a broad reflection at 22.5° to its (010) crystal plane and corresponding to a distance of 3.9 Å .The crystalline characteristics of these polymers appeared to be favorable for charge transport within PSCs.

Hole Mobility. Figure 6 displays the hole mobilities of the devices incorporating the pristine polymers and the Polymer/$PC_{61}BM$ blends with the blend ratio of 1:1 (w/w). The hole mobilities of the pristine **PTHBO**, **PBTTBO**, and **PTTTBO**

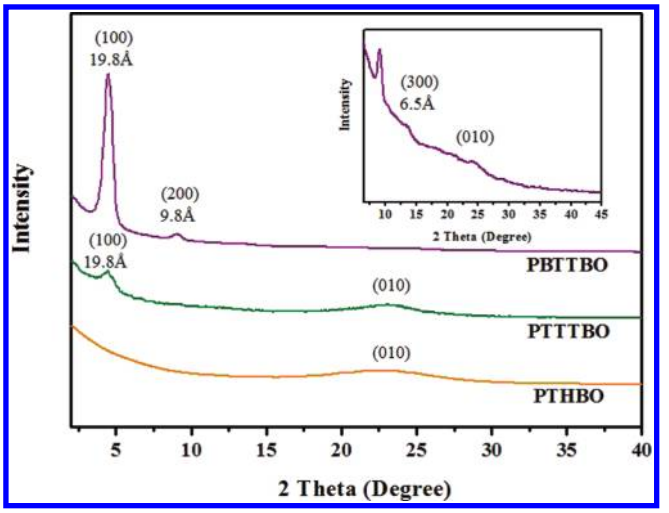

Figure 5. X-ray diffraction pattern of the pristine **PTHBO**, **PBTTBO**, and **PTTTBO** films.

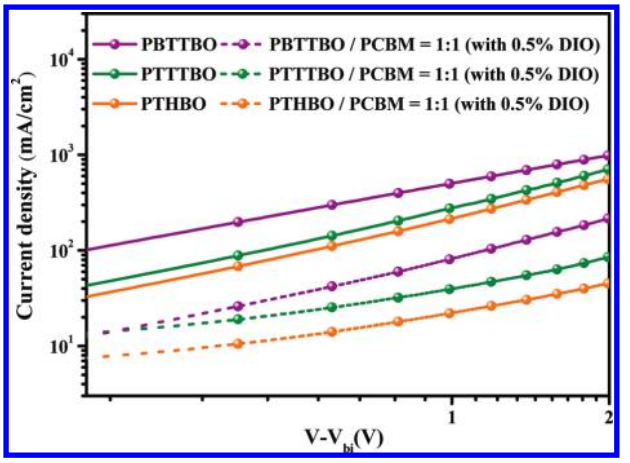

Figure 6. Dark $J-V$ curves for the hole-dominated carrier devices incorporating the pristine polymers and the blend films prepared at a blend ratio of 1:1 (w/w) with 0.5 vol % of DIO.

were 9.7×10^{-4}, 2.2×10^{-3}, and 1.2×10^{-3} $cm^2\ V^{-1}\ s^{-1}$, respectively while that of **PTHBO**, **PBTTBO**, and **PTTTBO** blends were 1.1×10^{-4}, 6.4×10^{-4}, and 2.5×10^{-4} $cm^2\ V^{-1}\ s^{-1}$, respectively. Thus, the hole mobility of the **PBTTBO** was greater than those of **PTHBO** and **PTTTBO**, presumably because of the greater crystallinity of **PBTTBO**.

Photovoltaic Properties. Next, we investigated the photovoltaic properties of the polymers in BHJ solar cells having the sandwich structure ITO/PEDOT:PSS/polymer:$PC_{61}BM$ (1:1, w/w)/Ca/Al, with the photoactive layers having been spin-coated from DCB solutions of the polymer and $PC_{61}BM$. The optimized weight ratio for the polymer and $PC_{61}BM$ was 1:1. In this case, we added a small amount of 1,8-diiodooctane (DIO; 0.5%, by volume relative to DCB) to optimize the miscibility of the blends. Figure 7 presents the $J-V$ curves of these PSCs; Table 4 summarizes the data. The devices prepared from polymer:$PC_{61}BM$ blends of **PTHBO**, **PBTTBO**, and **PTTTBO** exhibited open-circuit voltages (V_{oc}) of 1.02, 0.74, and 0.87 V, respectively; each value is related to the difference between the HOMO energy level of the polymer and the LUMO

energy level of $PC_{61}BM$.[48] We suspect that the **PBTTBO** blend provided the lowest value of V_{oc} because of its relatively higher-lying HOMO energy level. The short-circuit current densities (J_{sc}) of the devices incorporating **PTHBO**, **PBTTBO**, and **PTTTBO** were 8.3, 6.9, and 10.0 mA cm^{-2}, respectively. Furthermore, when we incorporated DIO (0.5 vol %) into the 1:1 (w/w) polymer:$PC_{61}BM$ blends, the devices based on **PTHBO**, **PBTTBO**, and **PTTTBO** exhibited slightly increased values of J_{sc} of 9.0, 7.9, and 11.6 mA cm^{-2}, respectively, resulting in increased PCEs. Figure 8 displays the EQE curves of the devices incorporating the polymer:$PC_{61}BM$ blends at weight ratios of 1:1 and 0.5 vol % DIO as the additive. These devices exhibited significantly broad EQE responses that extended into the visible range. We attribute these EQE responses in the visible region to the corresponding absorbances of the blends, resulting from both the intrinsic absorptions of the polymers and the presence of $PC_{61}BM$, which also absorbs significantly at 300−400 nm. In contrast, these devices displayed relatively lower EQE responses at wavelengths of greater than 700 nm because of the moderate absorbances of the polymer blends in this range. The device based on the **PTTTBO** blend exhibited the highest EQE response among our studied systems, with a maximum of 60% at 580 nm, consistent with its higher photocurrent. The theoretical short-circuit current densities obtained from integrating the EQE curves of the **PTHBO**, **PBTTBO**, and **PTTTBO** blends were 8.6, 7.5, and 11.1 mA cm^{-2}, values that agree reasonably with the measured (AM 1.5 G) values of J_{sc} of 9.0, 7.9, and 11.6 mA cm^{-2}, respectively, with a discrepancy smaller than 5%.

The higher FF value of the device incorporating **PBTTBO**:$PC_{61}BM$ (1:1, w/w) active layer with 0.5 vol % DIO as the additive is likely due to the higher hole mobility of the active layer, see Figure 6; the hole mobility of **PBTTBO** or **PBTTBO**:$PC_{61}BM$ (1:1, w/w) is larger than that of **PTHBO** and **PTTTBO** or **PTHBO**:$PC_{61}BM$ and **PTTTBO**:$PC_{61}BM$. Therefore, we attribute the enhanced FF to the increased hole mobility in the active layer, which is likely caused by the greater crystallinity in the **PBTTBO** active layer than in the **PTHBO** and **PTTTBO** active layer.[24] Notably, although **PBTTBO** had the best crystallinity and hole mobility, it provided the lowest value of J_{sc} among the three polymers. We attribute this lower value of J_{sc} to the low absorption coefficient (Figure 3c); consistently, the EQE curve also featured low EQE responses at 460−680 nm. Thus, more of the available photons from the solar radiation could be absorbed by **PTHBO** and **PTTTBO**, leading to the higher photocurrents of their devices.

Moreover, when exploring the decisive factors affecting the efficiencies of PSCs we must consider not only the absorption and energy levels of polymers but also the surface morphologies of the polymer blends. Figure 9 displays the surface morphologies determined through AFM measurements. Samples of the polymer:$PC_{61}BM$ blends were prepared using procedures identical to those used to fabricate the active layers of the devices. In each case, we observed a moderately homogeneous morphology of the polymer blends, except for the **PTHBO** blend, which displayed a coarse morphology. The root-mean-square roughness of **PTHBO**, **PBTTBO**, and **PTTTBO** were 9.3 nm, 3.8 and 3.1 nm, respectively (Figure 9a−c). The greater phase segregation and rougher surfaces of **PTHBO** blends presumably arose because of poor miscibility with $PC_{61}BM$, a

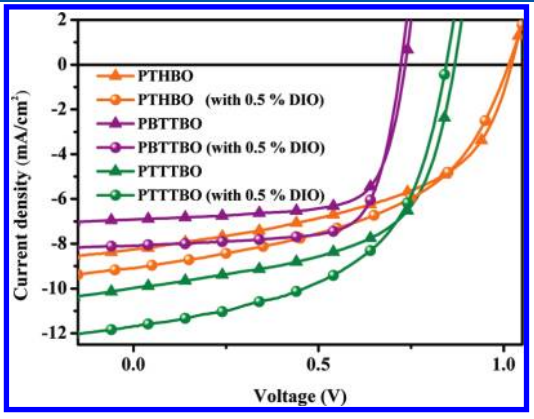

Figure 7. $J-V$ characteristics of PSCs incorporating polymer:$PC_{61}BM$ blends and with 0.5 vol % DIO additive, each prepared at a blend ratio of 1:1 (w/w).

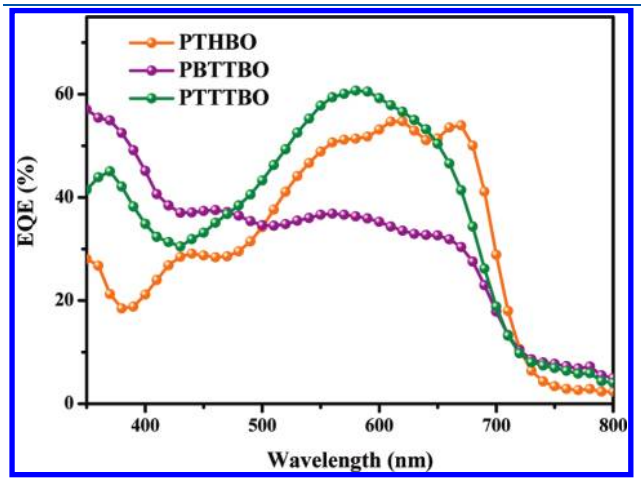

Figure 8. EQE curves of PSCs incorporating polymer:$PC_{61}BM$ blends and with 0.5% DIO additive, each prepared at a blend ratio of 1:1 (w/w).

Table 4. Photovoltaic Properties of PSCs Incorporating BO-Based Polymers

polymer/$PC_{61}BM$ (1:1) (w/w)	V_{oc} (V)	J_{sc} (mA cm^{-2})	FF (%)	PCE (%)	R_{sh} (Ω cm^2)	R_s (Ω cm^2)	thickness (nm)	mobility (cm^2 V^{-1} s^{-1})
PTHBO	1.02	8.3	51	4.2	445	15.2	82	
PTHBO[a]	1.02	9.0	49	4.5	564	21.5	95	1.1×10^{-4}
PBTTBO	0.74	6.9	72	3.7	1466	8.7	100	
PBTTBO[a]	0.72	7.9	74	4.2	1285	8.1	102	6.4×10^{-4}
PTTTBO	0.87	10.0	58	5.1	388	10.5	105	
PTTTBO[a]	0.85	11.6	54	5.3	450	10.8	100	2.5×10^{-4}

[a] Processed with 0.5 vol % DIO.

dx.doi.org/10.1021/ma201848z |*Macromolecules* 2011, 44, 9155–9163

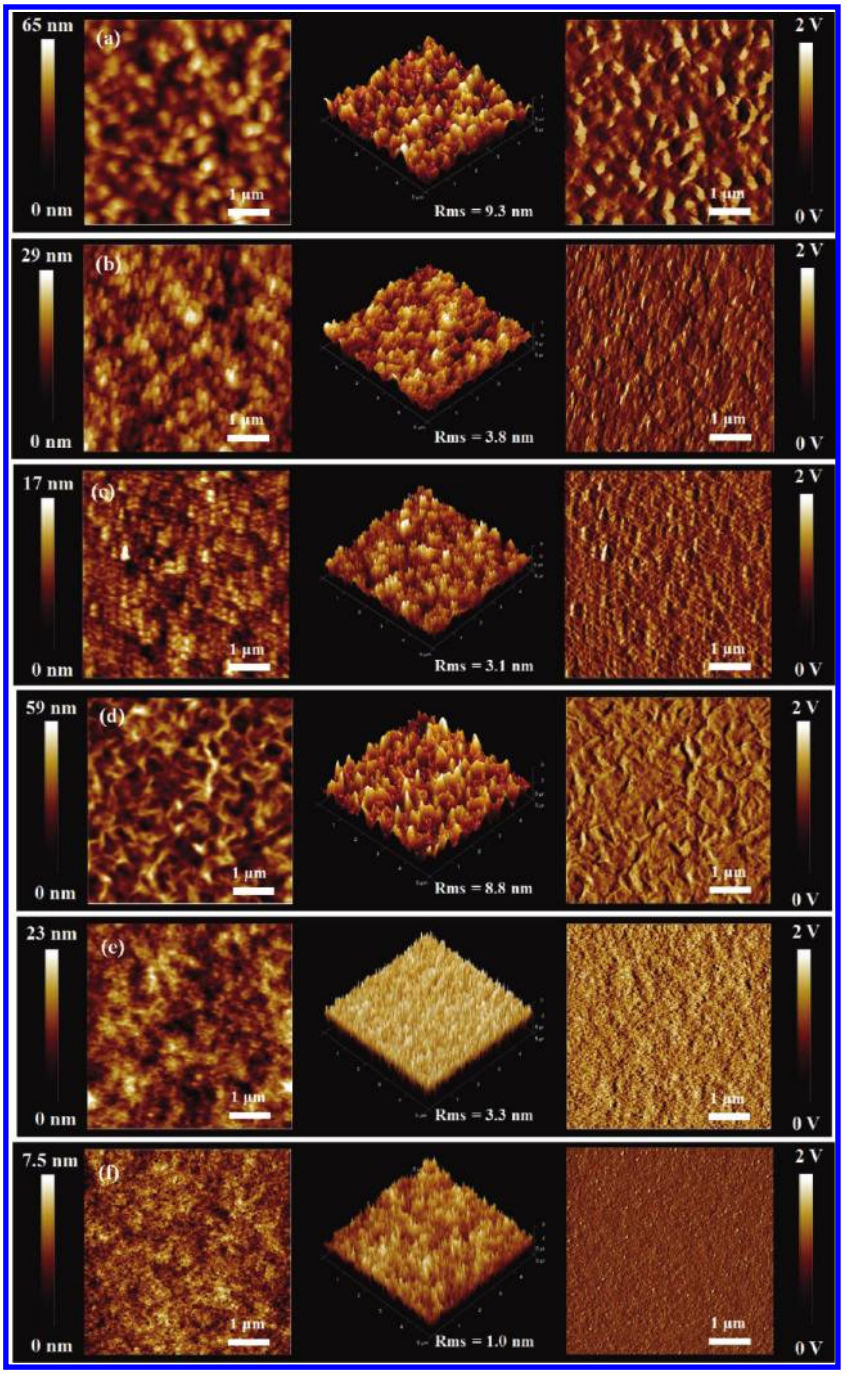

Figure 9. Topographic AFM images of polymer:$PC_{61}BM$ (1:1, w/w) blends incorporating (a) **PTHBO**, (b) **PBTTBO**, and (c) **PTTTBO** and with 0.5 vol % DIO additive for (d) **PTHBO**, (e) **PBTTBO**, and (f) **PTTTBO**.

result of the poor solubility of **PTHBO** compare with **PBTTBO** and **PTTTBO**. In contrast, Figure 9d to 9f display homogeneous morphology for the polymer/$PC_{61}BM$ blend films at weight ratios of the 1:1 that were processed with 0.5 vol % DIO additive, indicating that the incorporation of 0.5 vol % DIO optimized the miscibility of polymer chains with $PC_{61}BM$. The root-mean-square roughness of **PTHBO**, **PBTTBO**, and **PTTTBO** were 8.8, 3.3, and 1.0 nm, respectively (Figure 9d–f). Through optimization of the blend morphology, such high values of J_{sc} and PCE were also possible for the polymer:$PC_{61}BM$ blend at a weight ratio of 1:1.

CONCLUSIONS

We have used Stille coupling polymerization to prepare a series of new crystalline, conjugated polymers—**PTHBO, PBTTBO**, and **PTTTBO**—featuring alternating thiophene-based building blocks and benzooxadiazole (BO) units in their backbones. These polymers possess excellent crystallinity, thermal stability and low-lying HOMO energy levels. These desirable properties make **PTHBO, PBTTBO**, and **PTTTBO** promising materials for solar cell applications. A device incorporating **PTTTBO** and $PC_{61}BM$ (blend weight ratio, 1:1), with DIO (0.5 vol %) as an additive, exhibited a high value of V_{oc} of 0.87 V and a PCE of 5.3%.

AUTHOR INFORMATION

Corresponding Author
*E-mail: khwei@mail.nctu.edu.tw.

ACKNOWLEDGMENT

We thank the National Science Council, Taiwan, for financial support (NSC 98-2120-M-009-006).

REFERENCES

(1) Yu, G.; Gao, J.; Hummelen, J. C.; Wudl, F.; Heeger, A. J. *Science* **1995**, *270*, 1789.
(2) Wienk, M. M.; Koon, J. M.; Verhees, W. J. H.; Knol, J.; Hummelen, J. C.; van Hal, P. A.; Janssen, R. A. J. *Angew. Chem., Int. Ed.* **2003**, *42*, 3371.
(3) Dennler, G.; Scharber, M. C.; Brabec, C. J. *Adv. Mater.* **2009**, *21*, 1323.
(4) Chiu, M. Y.; Jeng, U. S.; Su, C. H.; Liang, K. S.; Wei, K. H. *Adv. Mater.* **2008**, *20*, 2573.
(5) Ma, W.; Yang, C.; Gong, X.; Lee, K.; Heeger, A. J. *Adv. Funct. Mater.* **2005**, *15*, 1617.
(6) Li, G.; Shrotriya, V.; Huang, J.; Yao, Y.; Moriarty, T.; Emery, K.; Yang, Y. *Nat. Mater.* **2005**, *4*, 864.
(7) Kim, Y.; Cook, S.; Tuladhar, S. M.; Choulis, S. A.; Nelson, J.; Durrant, J. R.; Bradley, D. D. C.; Giles, M.; McCulloch, I.; Ha, C. S.; Ree, M. *Nat. Mater.* **2006**, *5*, 197.
(8) Kim, J. Y.; Lee, K.; Coates, N. E.; Moses, D.; Nguyen, T. Q.; Dante, M.; Heeger, A. J. *Science* **2007**, *317*, 222.
(9) Bundgaard, E.; Krebs, F. C. *Sol. Energy Mater. Sol. Cells* **2007**, *91*, 954.
(10) Chen, G. Y.; Chiang, C. M.; Kekuda, D.; Lan, S. C.; Chu, C. W.; Wei, K. H. *J. Polym. Sci., Part A: Polym. Chem.* **2010**, *48*, 1669.
(11) Bijleveld, J. C.; Gevaert, V. S.; Nuzzo, D. D.; Turbiez, M.; Mathijssen, S. G. J.; de Leeuw, D. M.; Wienk, M. M.; Janssen, R. A. J. *Adv. Mater.* **2010**, *22*, E242.
(12) Yuan, M. C.; Chiu, M. Y.; Chiang, C. M.; Wei, K. H. *Macromolecules* **2010**, *43*, 6270.
(13) Chen, G. Y.; Cheng, Y. H.; Chou, Y. J.; Su, M. S.; Chen, C. M.; Wei, K. H. *Chem. Commun.* **2011**, *47*, 5064.
(14) Zhang, Y.; Hau, S. K.; Yip, H. L.; Sun, Y.; Acton, O.; Jen, A. K. Y. *Chem. Mater.* **2010**, *22*, 2696.
(15) Zhang, Y.; Zou, J.; Yip, H. L.; Sun, Y.; Davies, J. A.; Chen, K. S.; Acton, O.; Jen, A. K. J. *J. Mater. Chem.* **2011**, *21*, 3895.
(16) Jiang, J. M.; Yang, P. A.; Chen, H. C.; Wei, K. H. *Chem. Commun.* **2011**, *47*, 8877.
(17) Chang, Y. T.; Hsu, S. L.; Su, M. H.; Wei, K. H. *Adv. Mater.* **2009**, *21*, 2093.
(18) Chang, Y. T.; Hsu, S. L.; Chen, G. Y.; Su, M. H.; Sing, T. A.; Diau, E. W. G.; Wei, K. H. *Adv. Funct. Mater.* **2008**, *18*, 2356.
(19) Chang, Y. T.; Hsu, S. L.; Su, M. H.; Wei, K. H. *Adv. Funct. Mater.* **2007**, *17*, 3326.
(20) Huang, F.; Chen, K. S.; Yip, H. L.; Hau, S. K.; Acton, O.; Zhang, Y.; Luo, J.; Jen, A. K. Y. *J. Am. Chem. Soc.* **2009**, *131*, 13886.
(21) Chen, H. Y.; Hou, J. H.; Zhang, S. Q.; Liang, Y. Y.; Yang, G. W.; Yang, Y.; Yu, L. P.; Wu, Y.; Li, G. *Nat. Photonics.* **2009**, *3*, 649.
(22) Son, H. J.; Wang, W.; Xu, T.; Liang, Y. Y.; Wu, Y.; Li, G.; Yu, L. P. *J. Am. Chem. Soc.* **2011**, *133*, 1885.
(23) Chu, T. Y.; Lu, J.; Beaupre, S.; Zhang, Y.; Pouliot, J. R.; Wakim, S.; Zhou, J.; Leclerc, M.; Li, Z.; Ding, J.; Tao, Y. *J. Am. Chem. Soc.* **2011**, *133*, 4250.
(24) Price, S. C.; Stuart, A. C.; Yang, L.; Zhou, H.; You, W. *J. Am. Chem. Soc.* **2011**, *133*, 4625.
(25) Su, M. S.; Kuo, C. Y.; Yuan, M. C.; Jeng, U. S.; Su, C. J.; Wei, K. H. *Adv. Mater.* **2011**, *23*, 3315.
(26) Peet, J.; Kim, J. Y.; Coates, N. E.; Ma, W. L.; Moses, D.; Heeger, A. J.; Bazan, G. C. *Nat. Mater.* **2007**, *65*, 497.
(27) Blouin, N.; Michaud, A.; Gendron, D.; Wakim, S.; Blair, E.; Plesu, R. N.; Belletete, M.; Durocher, G.; Tao, Y.; Leclerc, M. *J. Am. Chem. Soc.* **2008**, *130*, 732.
(28) Scharber, M. C.; Mühlbacher, D.; Koppe, M.; Denk, P.; Waldauf, C.; Heeger, A. J.; Brabec, C. J. *Adv. Mater.* **2006**, *18*, 789.
(29) Bijleveld, J. C.; Shahid, M.; Gilot, J.; Wienk, M. M.; Janssen, R. A. J. *Adv. Funct. Mater.* **2009**, *19*, 3262.
(30) Hoven, C. V.; Dung, X. D.; Coffin, R. C.; Peet, J.; Nguyen, T. Q.; Bazan, C. C. *Adv. Mater.* **2010**, *22*, E63.
(31) Qin, P.; Li, W.; Li, C.; Du, C.; Veit, C.; Schleiermacher, H. F.; Andersson, M.; Bo, Z.; Liu, Z.; Inganas, O.; Wuerfel, U.; Zhang, F. *J. Am. Chem. Soc.* **2009**, *131*, 14612.
(32) Osaka, I.; Sauve, G.; Zhang, R.; Kowalewski, T.; McCullough, R. D. *Adv. Mater.* **2007**, *19*, 4160.
(33) Li, J.; Qin, F.; Li, C. M.; Bao, Q.; Chan-Park, M. B.; Zhang, W.; Qin, J.; Ong, B. S. *Chem. Mater.* **2008**, *20*, 2057.
(34) Rieger, R.; Beckmann, D.; Pisula, W.; Steffen, W.; Kastler, M.; Mullen, K. *Adv. Mater.* **2010**, *22*, 83.
(35) Li, Y.; Wu, Y.; Liu, P.; Birau, M.; Pan, H.; Ong, B. S. *Adv. Mater.* **2006**, *18*, 3029.
(36) Li, Y. W.; Li, Z. F.; Wang, C. Y.; Li, H.; Lu, H. G.; Xu, B.; Tian, W. J. *J. Polym. Sci., Part A: Polym. Chem.* **2010**, *48*, 2765.
(37) Melzer, C.; Koop, E. J.; Mihailetchi, V. D.; Blom, P. W. *Adv. Funct. Mater.* **2004**, *14*, 865.
(38) Zhou, E.; Wei, Q.; Yamakawa, S.; Zhang, Y.; Tajima, K.; Yang, C.; Hashimoto, K. *Macromolecules* **2010**, *43*, 821.
(39) Pommerehne, J.; Vestweber, H.; Guss, W.; Mahrt, R. F.; Bassler, H.; Porsch, M.; Daub, J. *Adv. Mater.* **1995**, *7*, 551.
(40) Liang, Y.; Feng, D.; Wu, Y.; Tsai, S. T.; Li, G.; Ray, C.; Yu, L. P. *J. Am. Chem. Soc.* **2009**, *131*, 7792.
(41) Zou, Y.; Gendron, D.; Neagu, R.; Leclerc, M. *Macromolecules* **2009**, *42*, 6361.
(42) Huo, L.; Hou, J.; Chen, H. Y.; Zhang, S.; Jiang, Y.; Chen, T. L.; Yang, Y. *Macromolecules* **2009**, *42*, 6564.
(43) Zhu, Y.; Champion, R. D.; Jenekhe, S. A. *Macromolecules* **2006**, *39*, 8712.
(44) Bredas, J. L.; Beljonne, D.; Coropceanu, V.; Cornil, J. *Chem. Rev.* **2004**, *104*, 4971.
(45) Thompson, B. C.; Frechet, J. M. *Angew. Chem., Int. Ed.* **2008**, *47*, 58.
(46) Scharber, M. C.; Muhlbacher, D.; Koppe, M.; Denk, P.; Waldauf, C.; Heeger, A. J.; Brabec, C. J. *Adv. Mater.* **2006**, *18*, 789.
(47) Wu, P. T.; Kim, F. S.; Champion, R. D.; Jenekhe, S. A. *Macromolecules* **2008**, *41*, 7021.
(48) Brabec, C. J.; Cravino, A.; Meissner, D.; Sariciftci, N. S.; Fromherz, T.; Rispens, M. T.; Sanchez, L.; Hummelen, J. C. *Adv. Funct. Mater.* **2001**, *11*, 374.